# HOKKAIDO UNIVERSITY

| | |
|---|---|
| Title | In situ monitoring of the growth of ice films by laser picosecond acoustics |
| Author(s) | Kashiwada, Saori; Matsuda, Osamu; Baumberg, Jeremy J. et al. |
| Citation | Journal of Applied Physics, 100, 073506<br>https://doi.org/10.1063/1.2353125 |
| Issue Date | 2006-10-01 |
| Doc URL | https://hdl.handle.net/2115/15423 |
| Rights | Copyright © 2006 American Institute of Physics |
| Type | journal article |
| File Information | JAP100-7.pdf |

# *In situ* monitoring of the growth of ice films by laser picosecond acoustics

Saori Kashiwada and Osamu Matsuda
*Graduate School of Engineering, Hokkaido University, Sapporo 060-8628, Japan*

Jeremy J. Baumberg
*School of Physics and Astronomy, University of Southampton, Southampton SO17 1BJ, United Kingdom*

Roberto Li Voti
*Dipartimento de Energetica, Università degli Studi di Roma "La Sapienza," Via A. Scarpa 16, 00161 Roma, Italy*

Oliver B. Wright[a)]
*Graduate School of Engineering, Hokkaido University, Sapporo 060-8628, Japan*

Ultrashort optical pulses are used to excite and probe picosecond acoustic pulses in a sample consisting of an opaque material upon which ice is continuously deposited from the vapor phase at ~110 K. By analysis of the ultrasonic propagation and reflection inside the submicron ice film and taking into account the scattering of the probe light by the acoustic waves, the thickness, sound velocity, refractive index, ultrasonic attenuation, and photoelastic constant of the ice film are derived. This method should find applications for the *in situ* monitoring of thin transparent films during growth. © *2006 American Institute of Physics*. [DOI: 10.1063/1.2353125]

## I. INTRODUCTION

Ice has remarkable physical properties due to the nature of the bonding between the constituent atoms and has been the subject of much attention in the physical and biological sciences. In particular, the dynamics of ice formation at temperatures below 150 K is important in astrophysics, being relevant to the study of comets, moons, or planetary rings, for example. In this temperature region ice is spontaneously formed by vapor deposition on cold substrates. The structure of ice films, for example, whether amorphous or crystalline, is highly dependent on the condensation temperature and condensation rate,[1] and much interest has been focused on growth mechanisms and film properties.[1–5]

Ultrasonic propagation and attenuation are particularly sensitive to material microstructure. However, it appears that there have been no ultrasonic studies in vapor-deposited ice to date. Such ice forms as a fragile thin-film structure, and it is not convenient for conventional ultrasonic measurements such as those making use of piezoelectric transducers. Thin submicron films can be conveniently studied using a noncontact and nondestructive method known as laser picosecond acoustics[6,7] in which ultrashort light pulses are used to excite and detect longitudinal acoustic pulses in thin films at frequencies typically in the 10 GHz–1 THz range. This technique has been applied to transparent thin films on opaque substrates for purposes of thickness and sound velocity measurements.[8] Here we extend this method not to derive only thickness and sound velocity but also to probe the ultrasonic attenuation and refractive index of the film. Furthermore, we apply this method to the *in situ* monitoring of the growth process of a vapor-deposited polycrystalline ice film at low temperatures.

We first discuss the experimental technique followed by the relevant theories for the generation, propagation, and optical detection of the acoustic strain pulses. We then present the experimental results and compare them with the theoretical predictions. We conclude by discussing future prospects for our approach.

## II. EXPERIMENTAL TECHNIQUE

The experimental arrangement is shown schematically in Fig. 1(a). An 800 nm opaque polycrystalline $YBa_2Cu_3O_{7-\delta}$ (YBCO with $\delta=0.16$) film with its *c* axis parallel to the growth direction is sputtered onto a (100) single-crystal MgO polished slab of thickness 0.5 mm. (This sample was obtained from THEVA GmbH.) This YBCO–MgO sample, serving as a substrate for the ice growth, is mounted in a liquid-nitrogen-cooled cryostat and is evacuated at room temperature using a rotary and turbomolecular pump combination. Figure 1(b) shows the thickness of the ice film that
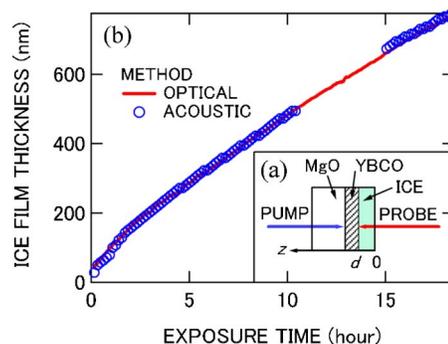


FIG. 1. (Color online) (a) Schematic diagram of the experimental setup. (b) Measured ice film thickness as a function of time at 110 K. The solid (red) line is obtained from the white light reflectance spectrum and the circles (blue) are obtained by laser picosecond acoustics.

[a)]Electronic mail: assp@kino-ap.eng.hokudai.ac.jp

forms on the YBCO surface at 110 K as a function on time, obtained by two different methods: (1) by an optical spectroscopic method and (2) by the use of laser picosecond acoustics, as explained later. At the deposition rates involved ($\sim$0.01 nm s$^{-1}$), cubic polycrystalline ice (Ic) is naturally formed at this temperature as a thin layer from the vapor phase owing to the presence of residual water vapor at a pressure of $\sim$0.1 mPa in the cryostat.[1,9] The microstructure of the YBCO film appears to favor ice nucleation while demonstrating convenient optical absorption properties for picosecond acoustic pulse generation and detection.

The optical source is a Ti:sapphire mode-locked laser with a central wavelength of 830 nm, a pulse duration of $\sim$100 fs, and a repetition rate of 82 MHz. Frequency-doubled pump light pulses of wavelength of 415 nm are focused at normal incidence onto the YBCO film to a spot diameter of $\sim$10 $\mu$m (full width at half maximum intensity) from the transparent MgO side to excite longitudinal acoustic pulses therein with a broad-frequency spectrum up to $\sim$20 GHz through the thermoelastic effect.[10] Because the acoustic wavelength, $\sim$300 nm, is much smaller than the spot diameter, one can consider the acoustic strain to propagate as plane waves along an axis parallel to the growth direction. With the ambient temperature at 110 K, the absorbed optical pump fluence per pulse of $\sim$0.2 mJ cm$^{-2}$ produces a maximum transient temperature rise of $\sim$45 K and a steady state temperature change of $\sim$1.2 K in the YBCO.[11] The YBCO substrate thickness is sufficient for the temperature of the ice film to remain close to 110 K. Normally incident probe light pulses of wavelength of 830 nm, with a fluence of $\sim$10% of the pump pulses, are focused on the opposite side of the sample to a spot diameter of $\sim$10 $\mu$m (full intensity width at half maximum) to monitor changes in optical reflectivity $R$ associated with the acoustic pulse propagation. Chopping the pump beam at 1 MHz permits the use of lock-in detection to give a resolution $\Delta R/R \sim 10^{-6}$ for a 50 Hz detection bandwidth. By scanning the time delay between the pump and the probe pulses in an optical delay line, time-resolved acoustic detection is possible with subpicosecond time resolution.

## III. MODELING THE ACOUSTIC STRAIN PULSE GENERATION AND PROPAGATION

In this section we describe a time-domain simulation of the strain pulse generation and propagation. The picosecond longitudinal strain pulse initially transmitted from the YBCO substrate to the ice film has a characteristic asymmetric exponential profile in the depth direction mirroring that of the optical absorption,[8] as shown by the theoretical curve on the far left in Fig. 2 obtained under the assumption of thermoelastic generation in the absence of thermal diffusion. The positive thermal expansion coefficient of YBCO (along the $c$ axis)[12] and the nearly equal acoustic impedances of YBCO and MgO lead to the strain being compressive (with a magnitude of $\sim 2 \times 10^{-4}$). The spatial extent of this strain profile is determined by the pump optical absorption depth in YBCO ($\sim$25 nm) and the longitudinal sound velocities $v$ and densities $\rho$ of ice and YBCO (see Table I). The values of $v$ and
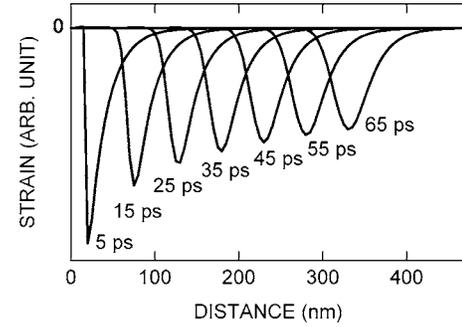


FIG. 2. Simulation of the longitudinal ultrasonic strain propagation in an ice film at 110 K assuming thermoelastic generation in YBCO in the absence of diffusion processes. The frequency dependence of the ultrasonic attenuation in the ice film is taken into account. The horizontal axis is in the $-z$ direction, and the zero of this axis is at the YBCO-ice boundary (at $z=d$).

$\rho$ for MgO are taken as 9598 m s$^{-1}$ and 3580 kg m$^{-3}$.[13] Frequency-dependent ultrasonic attenuation distorts this strain pulse as it propagates: we consider a quadratic frequency dependence, common to materials at ultrasonic frequencies in the gigahertz range and already noted in ice at lower frequencies.[14] (We have set the ultrasonic attenuation in the YBCO to zero because simulations of our data showed only marginal improvement when a finite quadratic frequency dependence was included.[15]) The propagation under these conditions can be accounted for with a simple numerical model for the longitudinal acoustic strain pulse $\eta(z,t)$ in the time domain, where $z$ is the coordinate opposite to the ice film growth direction (and where $z=0$ at the ice surface):
$\eta(z+v\,\delta t, t+\delta t) = (1-2a)\,\eta(z,t) + a\,\eta(z-v\,\delta t, t) + a\,\eta(z+v\,\delta t, t)$,
where $a$ is a constant coefficient and $\delta t$ is the time step used in the simulation. By expanding both sides of this expression to second order and treating the strain as a superposition of plane waves, $\eta(z,t) = \int A(k)\exp[i(kz-\omega(k)t)]dk$ ($k$ the acoustic wave number and $\omega$ the complex angular frequency), one obtains an equation involving an effective strain diffusion term:

$$\frac{\partial \eta}{\partial t} = -v\frac{\partial \eta}{\partial z} + a'v^2\frac{\partial^2 \eta}{\partial z^2}, \qquad (1)$$

where $a'=a\,\delta t$. This leads to the dispersion relation $\omega = vk - ia'v^2k^2$ and an ultrasonic attenuation coefficient $\alpha = (4\pi^2 a'/v)f^2 = bf^2$, where $f$ is the acoustic frequency and $b$ is a constant. The quantity $a'=a\,\delta t$ is chosen according to the value of $b$. Figure 2 shows the calculated strain pulse distribution [plotted as $\eta(z,t)$ as a function of $d$-$z$, where $d$ is the ice film thickness] in the ice film for a temperature of 110 K at various times using the value of $b$ taken from Table I and derived later in this paper. The strain pulse broadens as the higher-frequency components are preferentially absorbed (eventually becoming Gaussian in shape).

## IV. MODELING THE OPTICAL DETECTION OF STRAIN

We now describe the model used for the optical reflectivity changes. The transient complex amplitude-reflectance change for an arbitrary strain distribution in a transparent

TABLE I. Physical constants for ice and YBCO. The definitions of the symbols are as follows: $\nu$ is the longitudinal sound velocity, $\rho$ is the mass density, $C$ is the specific heat capacity, $n+ik$ is the complex refractive index, $\lambda$ is the optical wavelength, $\zeta$ is the optical absorption depth, $dn/d\eta$ and $dk/d\eta$ are photoelastic constants, and $b$ is the coefficient involved in the ultrasonic attenuation that varies quadratically with the acoustic frequency ($\alpha=bf^2$). The symbols $n'$, $k'$, $\zeta'$, and $\lambda'$ refer to the pump light, whereas $n$, $k$, $\zeta$, and $\lambda$ refer to the probe light. The density and longitudinal sound velocity for YBCO at both 110 and 300 K are taken to be equal to those quoted in Ref. 18 at 80 K.

| | Ice (110 K) | | YBCO (110 K) | | YBCO (300 K) |
| --- | --- | --- | --- | --- | --- |
| | Ref. | Fit | Ref. | Fit | Fit |
| $v$ (m s$^{-1}$) | 3592[a] | 3510 | 5400[b] | ... | 5400[b] | ... |
| $\rho$ (kg m$^{-3}$) | 930[c] | ... | 6350[b] | ... | 6350[b] | ... |
| $C$ (J kg$^{-1}$ K$^{-1}$) | ... | ... | 200[d] | ... | 260[d] | ... |
| $n'+ik'$ at $\lambda'=415$ nm | ... | ... | $1.51+1.35i$[e] | ... | $1.51+1.35i$[e] | ... |
| $n+ik$ at $\lambda=830$ nm | 1.31[f] | 1.30 | $1.28+1.38i$[e] | ... | $1.28+1.38i$[e] | ... |
| $\zeta'=\lambda'/4\pi k'$ (nm) at $\lambda'=415$ nm | ... | ... | 24.5 | ... | 24.5 | ... |
| $\zeta=\lambda/4\pi k$ (nm) at $\lambda=830$ nm | ... | ... | 56.5 | ... | 56.5 | ... |
| $dn/d\eta$ at $\lambda=830$ nm | ... | −0.084 | ... | 0.41 | ... | 2.0 |
| $dk/d\eta$ at $\lambda=830$ nm | ... | 0 | ... | −0.05 | ... | −0.25 |
| $b$ ($\mu$m$^{-1}$ GHz$^{-2}$) | 0.0027[g] | 0.002 | ... | 0 | ... | 0 |

[a]Reference 19.
[b]Reference 13.
[c]Reference 20.
[d]Reference 18.
[e]Reference 21.
[f]Reference 22.
[g]Reference 14.

layer (ice) on an opaque substrate (YBCO) can be expressed in a concise form, fully accounting for multiple optical reflections:[16,17]

$$\frac{\delta r}{r} = \frac{ik_0}{2a_0b_0}\left\{ \int_0^d \Delta\varepsilon_1(z')[a_1\exp(ik_1z')+b_1\exp(-ik_1z')]^2dz'\right.$$

$$+\int_0^\infty \Delta\varepsilon_2(z'+d)a_2^2\exp(2ik_2z')dz'$$

$$\left.+(a_1+b_1)^2(1-\varepsilon_1)u(0)+a_2^2(\varepsilon_1-\varepsilon_2)u(d)\right\}. \qquad (2)$$

where

$$a_0=(k_0+k_1)(k_1+k_2)+(k_0-k_1)(k_1-k_2)\exp(2ik_1d),$$

$$b_0=(k_0-k_1)(k_1+k_2)+(k_0+k_1)(k_1-k_2)\exp(2ik_1d),$$

$$a_1=2k_0(k_1+k_2),$$

$$b_1=2k_0(k_1-k_2)\exp(2ik_1d),$$

$$a_2=4k_0k_1\exp(ik_1d).$$

Here $u(z)$ is the $+z$-directed displacement, $\varepsilon_i=\tilde{n}_i^2$ are dielectric constants (with $\tilde{n}_i=n_i+i\kappa_i$ the probe complex refractive index), $k_i$ are optical wave numbers, $\Delta\varepsilon_i=2\tilde{n}_i\eta(z,t)d\tilde{n}_i/d\eta$ are dielectric constant changes caused by the photoelastic effect, and $i=0,1,2$, refer to the low-pressure vapor, ice, and YBCO, respectively. The integrals arise because of the spatially smeared changes in refractive index. The presence of the MgO substrate in Eq. (2) has been neglected because a negligible amount of probe light reaches the YBCO–MgO

interface. It is evident that changes in $r$ are induced both by the photoelastic effect (changes in refractive index associated with strain in both the ice and the YBCO) and by surface $[u(0)]$ or interface $[u(d)]$ displacements. The relative reflectivity variation measured in experiment is given by $\Delta R(t)/R=2\,\mathrm{Re}(\delta r/r)$.

## V. EXPERIMENTAL RESULTS AND DISCUSSION

We now compare the predictions of Eq. (2) with the experimental results: the solid (red) curves in Fig. 3(a) show the measured $\Delta R/R$ variations for ice film thicknesses of 129 and 773 nm at 110 K. The typical magnitude of $\Delta R/R$ is $\sim 10^{-4}$. These data are obtained by one scan of the optical
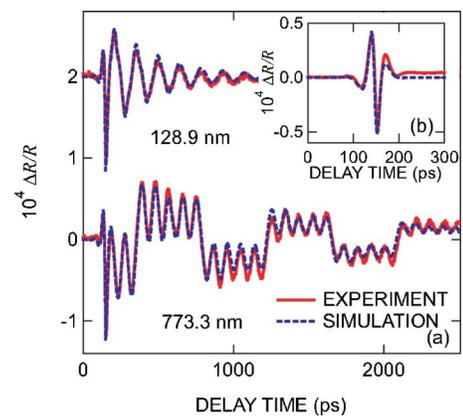


FIG. 3. (Color online) Relative reflectivity changes $\Delta R/R$ as a function of delay time: (a) for ice films at 110 K of thicknesses of 129 and 773 nm on an 800 nm YBCO film and (b) for the bare YBCO film at 300 K. The solid (red) lines represent experimental data and the dashed (blue) lines are theoretical fits.

delay line. The dashed (blue) curves in Fig. 3(a) are theoretical fits using the above theory and parameters taken from Table I. The density ($\rho_1$) of the ice film is taken as the literature value for Ic, whereas the film thickness, the longitudinal sound velocity ($v_1$), the refractive index ($n_1$), the ultrasonic attenuation (constant $b$), and the photoelastic constant ($dn_1/d\eta$) of the ice are fitted using the complete data set for the growing ice film. (A constant scale factor, independent of film thickness, is used to match the amplitude of the fits with the data.) How the thickness, sound velocity, and refractive index of the ice can be fitted simultaneously is explained later in this paper. The agreement between experiment and theory is seen to be very good. The sharp downward spike at around 150 ps corresponds to the strain pulse arrival at the YBCO-ice interface, and in this time domain $\Delta R$ is mainly determined by the photoelastic effect in YBCO [the second term in Eq. (2)] into which the probe light penetrates by $\sim 50$ nm. The subsequent oscillations of frequency of $\sim 10$ GHz in the $d = 773$ nm data arise through the photoelastic effect in the ice [the first term in Eq. (2)]; the strain pulse behaves like a moving mirror, producing interference with the probe light reflected from the YBCO-ice interface. The oscillation period is given by $\tau_1 = \lambda/2n_1 v_1 \sim 100$ ps, where $\lambda$ is the optical wavelength of the normally incident probe light.[7,17] Superimposed on this variation are periodic steps, of period $\tau_2 = 2d/v_1$, caused mainly by the surface motion [the term involving $u(0)$ in Eq. (2)] associated with the strain pulse being reflected from the ice film surface.[8] This period $\tau_2$, increasing with increasing ice film thickness, coincides with the round-trip time of the strain pulse in the ice film. (Steps arising primarily from the ice-YBCO interface motion, much smaller than those corresponding to the surface motion owing to presence of the YBCO, can hardly be resolved.) In the $d = 129$ nm data this contribution with period $\tau_2$ is dominant. For comparison we show in Fig. 3(b) the measured and fitted $\Delta R/R$ variations for the bare YBCO surface at room temperature. The variation is different from the corresponding portions of $\Delta R(t)/R$ (between 100 and 200 ps) measured at low temperatures because of the temperature dependence of the photoelastic constants $dn_2/d\eta$ and $d\kappa_2/d\eta$ and the absence of the ice film at room temperature (see Table I).

An overall comparison of experiment and theory can be obtained from a density plot of $\Delta R(t)/R$ as a function of growth time up to 18 h, as shown in Figs. 4(a) and 4(b), respectively. Delay line scans are obtained every 10 min for up to 18 h. The optical pump light was turned off during the period of 10.5–15 h to verify that this had no effect on the growth process. By monitoring the optical spectrum of a beam of white light reflected at normal incidence from the ice film side of the sample throughout the growth process and fitting the results using a standard optical multiple reflection analysis at a wavelength of 830 nm (assuming a constant value for $n_1 = 1.30$ from Table I), we were able to determine the thickness variation of the film over the whole measurement period. As shown in Fig. 1, this purely optical measurement is consistent with the picosecond acoustic measurement. The evident excellent agreement between theory and experiment using a unique set of fitting parameters over
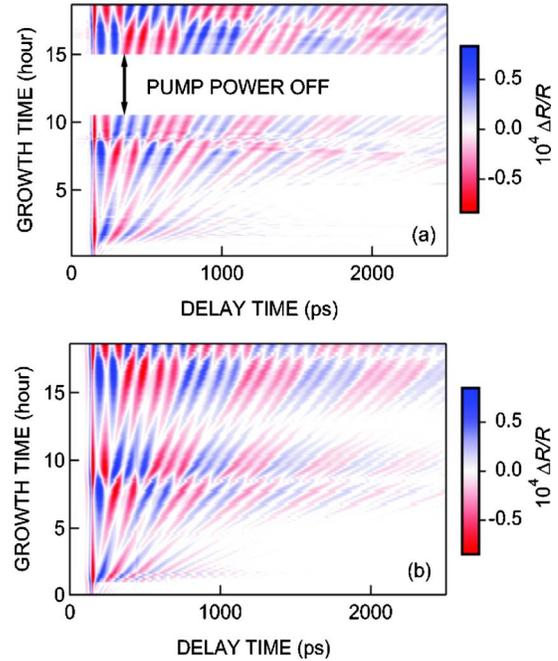


FIG. 4. (Color online) Density plot of $\Delta R(t)/R$ for the ice film growth at 110 K over a period of 18 h: (a) experiment and (b) theoretical simulation.

the whole growth process suggests that the properties of the ice film do not vary significantly with thickness. [The comparison of experiment and theory in Fig. 4 can also be effectively done by viewing an animation of the reflectivity changes as a function of time.[23] The sign flips of the steps in this animation arise mainly through the variation in $a_0$ in Eq. (2) and to a good approximation occur when the film thickness changes by integral multiples of $\lambda/4n \approx 160$ nm.] In particular the decay in $\Delta R(t)/R$ allows the ultrasonic attenuation constant to be determined as $b = 0.002 \pm 0.0005$ $\mu m^{-1}$ GHz$^{-2}$ for the vapor-deposited ice film. These measurements at $\sim 10$ GHz, giving $\alpha \approx 0.2$ $\mu m^{-1}$, represent the highest frequency measurements to date of the ultrasonic attenuation in ice.[24] We have not been able to find data on cubic ice for comparison, but lower-frequency measurements below 150 MHz on single-crystal hexagonal ice at 100 K (obtained from the liquid phase) give an ultrasonic attenuation consistent with an $f^2$ variation for $\alpha$, with a similar value of $b = 0.0027$ $\mu m^{-1}$ GHz$^{-2}$ in the relation $\alpha = bf^2$.[14] However, without a knowledge of the microstructure or grain size of our films it is difficult to determine the origin of the ultrasonic attenuation in our films. Our fitted values for the sound velocity and refractive index of vapor-deposited ice, $v_1 = 3510 \pm 100$ m s$^{-1}$ and $n_1 = 1.30 \pm 0.05$, are also in close agreement with literature values for hexagonal ice (Ih) (3592 m s$^{-1}$ and 1.31). The photoelastic constant of vapor-deposited ice relevant to the present experiment is determined as $P_{12} = 2n_1 dn_1/d\eta = -0.084 \pm 0.02$ (at 830 nm). We do not know of any comparable measurements. Other materials that have been found to have a negative value of $P_{12}$ at optical frequencies are GaP and GaAs.[25]

As mentioned above, for measurements at a single angle of incidence for transparent films one has access to two characteristic times. For normal probe incidence these are $\tau_1$
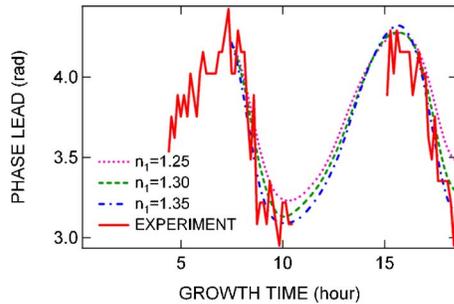
FIG. 5. (Color online) Phase lead of the oscillations in reflectivity at ~10 GHz (with respect to a sine variation with the origin at $t=145$ ps, just after the time of arrival of the acoustic pulse at the YBCO-ice interface). The solid (red) line represents the experimental data whereas the dotted (purple), dashed (green), and dashed-dotted (blue) lines represent theoretical fits for three different values of the refractive index $n_1$ of the ice film (holding the parameters $\tau_1$ and $\tau_2$ constant). The best agreement is obtained when $n_1 = 1.30$.

$=\lambda/2n_1v_1$, the period of the oscillations arising from the photoelastic effect, and $\tau_2=2d/v_1$, the period of the steps in $\Delta R/R$ caused by surface and interface motion. It is not possible to obtain the three quantities $d$, $v_1$, and $n_1$ from just two measured quantities.[8] However, the phase of the photoelastic oscillations of period $\tau_1$ is sensitive to the precise value of $n_1$ as is evident by the presence of the complex wave number $k_1$ (dependent on $n_1$) in Eq. (2). Although for a single film thickness it is impractical to attempt to accurately fit the three quantities $d$, $v_1$, and $n_1$, the use of a whole data set of the same material with different film thicknesses allows this to be done. As an illustration of this effect we show in Fig. 5 the experimental phase lead (with respect to a sine variation measured from the signal onset time at 145 ps) of the photoelastic oscillations as a function of film thickness together with the theoretical predictions for this phase lead for two different values of $n_1$ around the optimal value, holding the parameters $\tau_1$ and $\tau_2$ constant (while varying $d$ and $v_1$ accordingly). The deviations in the phase for different values of $n_1$ are evident. In particular, at a growth time of 10 h, corresponding to a film thickness of ~450 nm, the sensitivity of the phase lead to $n_1$ becomes enhanced. Due to the optical interference effects inherent in Eq. (2), this sensitivity is a periodic function of the ice film thickness (with period $\lambda/2n_1 \approx 320$ nm).

As a check on the composition of the deposited films we performed an additional experiment by introducing deionized water into the cryostat from outside using a needle value until the pressure reached ~0.7 Pa.[26] The results for the reflectivity variation for an ice film at 95 K for a single thickness of ~630 nm are shown in Fig. 6, corresponding to a similar deposition rate as in the above experiments. The structure of the ice is again expected to be polycrystalline (Ic).[1] The photoelastic oscillation frequency is seen to be identical to that measured in the previous set of experiments, supporting our assertion that we are indeed observing ice films. The oscillations die out after ~350 ps, possibly because of the formation of a rough outer surface on the ice film for the higher pressure involved in this experiment.[26]
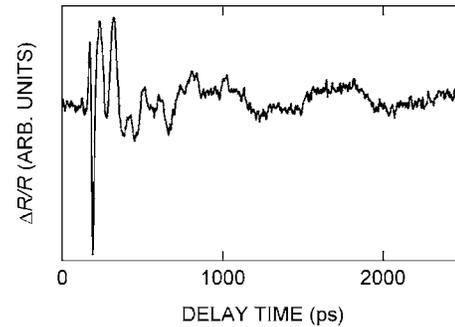


FIG. 6. Relative reflectivity change $\Delta R(t)/R$ obtained when water is introduced into the vacuum chamber intentionally to form ice. These data correspond to an ice film thickness of ~630 nm at a temperature of 95 K.

## VI. CONCLUSIONS

In conclusion, we have succeeded in the generation and detection of picosecond acoustic pulses in vapor-deposited ice films at low temperatures. The data can be understood with a model based on thermoelastic generation and optical detection accounting for optical interference effects in the transparent film. This work also demonstrates that laser picosecond acoustics can be used for the *in situ* monitoring of transparent thin film growth. The ability to extract the ultrasonic attenuation, in particular, should prove useful in the evaluation of the microstructure of thin films during the growth process.

In the future it would be useful to obtain results at two or more different probe angles of incidence in order to provide a further check on the film thickness, refractive index, and sound velocity.[27] It would also be interesting to investigate the effect of growth rate on the physical properties of the ice films. One might expect an increase in ultrasonic attenuation with growth rate, for example, that could be correlated with the film structure.

[1]A. Kouchi, T. Yamamoto, T. Kuroda, and J. M. Greenberg, Astron. Astrophys. **290**, 1009 (1994).
[2]D. E. Brown, S. M. George, C. Huang, E. K. L. Wong, K. B. Rider, R. S. Smith, and B. D. Kay, J. Phys. Chem. **100**, 4988 (1996).
[3]A. Kouchi, Nature (London) **330**, 550 (1987).
[4]S. Mitlin and K. T. Leung, J. Phys. Chem. B **106**, 6234 (2002).
[5]H. Bluhm and M. Salmeron, J. Chem. Phys. **111**, 6947 (1999).
[6]C. Thomsen, H. T. Grahn, H. J. Maris, and J. Tauc, Phys. Rev. B **34**, 4129 (1986).
[7]T. Saito, O. Matsuda, and O. B. Wright, Phys. Rev. B **67**, 205421 (2003).
[8]O. B. Wright, J. Appl. Phys. **71**, 1617 (1992).
[9]R. E. Honig and H. O. Hook, RCA Rev. **21**, 360 (1960).
[10]The deformation potential of YBCO is not expected to contribute significantly to the acoustic generation because of the subpicosecond relaxation time of carriers.
[11]The maximum transient temperature rise can be estimated using the expression $Q(1-R)/(AC\zeta')$, where $Q$ is the energy of a single incident optical pump pulse, $R$ is the optical reflectance of the pump beam from the

sample, $A = \pi w^2/2$ is the pump beam spot area, $C$ is the specific heat per unit volume of YBCO, and $\zeta'$ is the optical penetration depth of the pump beam in YBCO. The spot radius $w = 8.5 \ \mu$m is obtained from the pump beam lateral intensity profile, given by $I(r) = I_0 \exp(-2r^2/w^2)$. There is a simple relation between $w$ and the full intensity width at half maximum $D$ in this case: $w = D/\sqrt{2 \ln 2} \approx 0.85D$. In our case $Q(1-R)$ is equal to 0.16 nJ. The steady state temperature rise of the sample at the center of the optical pump spot can be estimated from the expression $P(1-R)/(\sqrt{2\pi}w\kappa)$, where $P$ is the average power of the (chopped) optical pump beam and $\kappa$ is the thermal conductivity of the MgO substrate. The presence of the ice film and YBCO has a negligible effect on this steady state temperature rise. In our case $P(1-R)$ is equal to 6.6 mW. The value of $\kappa$ was taken from Y. S. Touloukian, *Thermophysical Properties of Matter: Thermal Conductivity-Nonmetalic Solids* (Plenum, New York, 1970), Vol. 2, p. 158. The value of $C$ was taken from Ref. 18. The refractive index of MgO at 415 nm was taken to be equal to 1.76, obtained from E. D. Palik and G. Ghosh, *Electronic Handbook of Optical Constants of Solids* (Academic, San Diego, 1999).

[12]M. Zeisberger, I. Latka, W. Ecke, T. Habisreuther, D. Litzkendorf, and W. Gawalek, Supercond. Sci. Technol. **18**, S202 (2005).

[13]C. Elbaum, J. Phys. IV **6**, C8–445 (1996).

[14]J. Tatibouet, R. Vassoille, and J. Perez, J. Glaciol. **15**, 161 (1975).

[15]The optimum value of $b$ for YBCO at 110 K was found to be $b = 0.000 \ 13 \ \mu$m$^{-1}$ GHz$^{-2}$. Including this in the fitting only reduced the re-siduals by $\sim 15\%$. This attenuation affects only the initial portion of the variation in $\Delta R/R$ when the acoustic pulse is first transmitted to the ice film from the YBCO film.

[16]H.-N. Lin, R. J. Stoner, H. J. Maris, and J. Tauc, J. Appl. Phys. **69**, 3816 (1991).

[17]O. Matsuda and O. B. Wright, J. Opt. Soc. Am. B **19**, 3028 (2002).

[18]M. Lang *et al.*, Z. Phys. B: Condens. Matter **69**, 459 (1988).

[19]W. P. Mason, *Physical Acoustics and the Properties of Solids* (Van Nostrand, Princeton, NJ, 1958).

[20]V. F. Petrendo and R. W. Whitworth, *Physics of Ice* (Oxford, New York, 1999), p. 256.

[21]I. Bozovic *et al.*, Phys. Rev. B **38**, 5077 (1988).

[22]http://www.icess.ucsb./edu/hydro/aviris/optics.html

[23]See http://kino-ap.eng.hokudai.ac.jp or EPAPS Document No. E-JAPIAU-100-247618 for the animation. This document can be reached via a direct link in the online article's HTML reference section or via the EPAPS homepage (http//www.aip.org/pubservs/epaps.html).

[24]$\Delta R/R$ is dominated by contributions from acoustic waves of frequency $1/\tau_1 \approx 10$ GHz. Hence the fitting of the ultrasonic attenuation is not sensitive to the particular frequency dependence for $\alpha$ assumed.

[25]R. W. Dixon, J. Appl. Phys. **38**, 5149 (1967).

[26]The larger pressure here is thought to be due to the presence of dissolved air in the introduced de-ionized water.

[27]R. Cote and A. Devos, Rev. Sci. Instrum. **76**, 053906 (2005).